Effect of Ultrasonication on the Solidification Microstructure in Al and Mg-Alloys

X. Zhang[1], H.R. Kotadia[2], J. Depner[1], M. Qian[3] and A. Das[1, *]
[1]College of Engineering, Swansea University, Bay Campus, Swansea, SA1 8EN, UK
[2]Warwick Manufacturing Group, University of Warwick, Coventry, CV4 7AL, UK
[3]Centre for Additive Manufacturing, School of Engineering, RMIT University, Melbourne, Australia
[*]e-mail: A.Das@swansea.ac.uk

Abstract:
Solidification microstructures formed under high-intensity ultrasonication are systematically investigated in various Al and Mg-alloys. The range of microstructures examined include primary grain structure, intermetallic compounds (IMCs), regular and irregular eutectics. Extensive grain refinement is observed in all alloys, especially in the areas of cavitation, further facilitated by the presence of solute. Heat treatability of the ultrasonicated alloys is enhanced as the fine-grained microstructure reduced diffusion distance. Regular lamellar eutectic microstructure is observed to degenerate under cavitation. Irregular eutectic and IMCs are modified from coarse plates or complex morphology into compact polygonal shape. Result suggests that ultrasonication increases nucleating particles and potency of nucleants. The modification of eutectic and IMCs predominantly occurs through coarsening and spheroidisation in the area of intense cavitation. While grain refinement effect is noticed in the entire ingots assisted by acoustic streaming, eutectic modification effect dissipates rapidly outside the area of cavitation.

Keywords: Ultrasound; Cavitation; Grain refinement; Eutectic; Artificial aging; Light alloys.

Introduction

The demand and use of light metals and alloys have greatly increased in structural applications. Al and Mg-based alloys are particularly attractive for a range of applications including structural, automotive, aerospace, biomedical and electronics primarily due to their low density and high specific-strength. However, one major drawback of such alloys is their poor absolute strength in the as-cast condition compared to ferrous alloys. Controlling the solidification microstructure is the most fundamental approach to enhance the mechanical performance, cast quality and downstream processability of such light alloys [1]. In most Al and Mg-based alloys, solidification microstructure is complex and multi-phase in nature consisting of primary grains, intermetallic compounds (IMC) and eutectic. Therefore, understanding the formation of such microstructure and designing methods to modify it during solidification is of tremendous scientific and technological importance. Chemical modification of microstructure during solidification such as, chemical grain refinement of Al-alloys using Al-Ti-B master alloys [2,3] and Mg-alloys using Zr [4,5] or modification of eutectic in Al-Si alloys with minor addition of Na or Sr [6] is well-established and widely practiced. However, chemical methods have several limitations. Most importantly, their effectiveness depends on the alloy system as many established refiners are susceptible to ‘poisoning’ from specific alloying elements [7], for example, Al-Ti-B in Al-Si and Zr in Mg-Al alloys. Eutectic modifiers, on the other hand, do not refine the grain structure and are linked with possible casting defects.

Physical modification of solidification microstructure can address the inherent limitations of chemical methods and are applicable irrespective of alloys constitution. Most physical method rely on creating intensive agitation in the melt to alter the nucleation and growth behaviour of solid. Several methods, such as physical melt shearing [8], electromagnetic stirring [9] or electric pulse [10] have been widely investigated, though application of ultrasound during solidification [11] appears to be the most promising of such physical methods. One of the major benefits of ultrasonication stems from its ability to alter different phases making it suitable for controlling the complex solidification microstructures in light alloys. Primary grain refinement in Al [12-14] and Mg-alloys [15-17] as well as modification of eutectic and intermetallic phases have been reported in Al-Si alloys [18,19]. However, understanding of the mechanism of microstructure modification under ultrasonication is yet to be comprehensive. While it's well-accepted that microstructure modification originates from cavitation (shockwave generation through formation and violent collapse of bubbles in the melt) and acoustic streaming (large-scale fluid flow from attenuation of ultrasound) effects [11], the contributions from nucleation, particle fragmentation and coarsening are still debated. Further investigation is necessary for developing a comprehensive understanding of ultrasound induced microstructure modification and identifying the capabilities and application regimes of such methods.

This paper presents an overview of our work on microstructure modification in Al and Mg-alloys using ultrasonication. This covers experimental evidence on grain refinement and its influence on the heat treatability of the alloy, effect of solute on the grain refinement potential, and modification of eutectic and intermetallic phases. Finally, mechanism behind the microstructure modification is suggested.

Experimental

Compositions of Al and Mg-alloys investigated are reported in table 1. The alloys were melted and homogenised at 725-750 ^{o}C in clay graphite crucibles in an electric resistance furnace. The molten alloys were taken out and ultrasonicated at 20 kHz frequency and 25 μm amplitude for ~ 420 s (till near the end of solidification) using a 25 mm dia Ti-6Al-4V (all compositions expressed in wt.%) radiator introduced below the surface of the melt. The radiator was preheated (~ 400 ^{o}C) by ultrasonicating a batch of discarded melt first to avoid any chill effect. Alloy samples were also solidified under identical cooling arrangement but without ultrasonication for comparison. Solidified ingots (height 60–80 mm, diameter 50 mm) were sectioned along the central vertical plane and ground and polished using standard metallographic techniques. Al-Cu samples were anodized using Barker's reagent (7 ml 48% HBF_4 in 200 ml distilled water) at 20 V DC for 70 s using a stainless-steel cathode, while Al-Si were unetched. Mg-Alloy samples were chemically etched in Acetic Glycol (20 ml Acetic Acid, 1 ml HNO_3, 60 ml Ethylene Glycol, 20ml Water) for 15-30 s. A Zeiss Axioscope microscope was used for microstructural examination and linear intercept method was used for grain size measurement considering over 250 grains for each measurement. The AZ80 alloy samples were solution treated for 6 h at 400 ^{o}C followed by quenching in water. Solution treated samples were artificially aged at 150, 200 and 225 ^{o}C for times varying between 1-16 h followed by quenching in water. Vickers hardness measurement was conducted for individual

samples in an Innovatest hardness tester using 1 kgf under 10 s dwell time. Average hardness data were calculated from 5-10 individual measurements.

Table.1. Chemical compositions of alloys investigated.

Alloy	Composition (wt.%)							
	Mg	Al	Zn	Si	Mn	Cu	Fe	Sr
Al-33Cu		Bal-		0.04		32.6	0.15	
Al-16Si		Bal-		16.1	0.16		0.37	
AZ31	Bal-	3.0	1.0		0.6			
AZ80	Bal-	8.5	0.5		0.31			
AZ91	Bal-	9.0	0.5		0.3			
AJ62	Bal-	6.1	0.2		0.36			2.5

Results

Solidification microstructure of primary phase grains

Microstructures from Mg-alloy ingots solidified under identical cooling conditions with and without ultrasonication are presented in Fig. 1. In the absence of ultrasonication, the primary phase grain structure is predominantly dendritic in nature (Figs. 1a,c,e) with some of the dendrite arms long enough to span the entire field of view. Microstructures from the top of the ultrasonicated ingots (just below the radiator) show drastically refined and equiaxed grain structure as evidenced in Figs. 1b,d,f. Such transformation to refined equiaxed grain structure is evidenced in all alloy systems investigated highlighting the universal nature of grain refinement under ultrasonication irrespective of alloy constitution. A gradual increase in the grain size was observed in all alloy samples with increasing distance from the ultrasound radiator. Nevertheless, for the size of ingots investigated, the entire ingot microstructure consisted of non-dendritic grains and the largest observed grain size under ultrasonication was still significantly finer than the size of the dendrites formed under conventional solidification. This highlights the influence of cavitation in grain refinement under ultrasonication whereby the refinement effect is strongest near the radiator, the area of active cavitation. Although reduction in cavitation deteriorates the refinement potential with distance from the radiator, dispersion of nuclei and grains from the area of cavitation into the bulk melt through acoustic streaming leads to the overall equiaxed microstructure in the ingots.

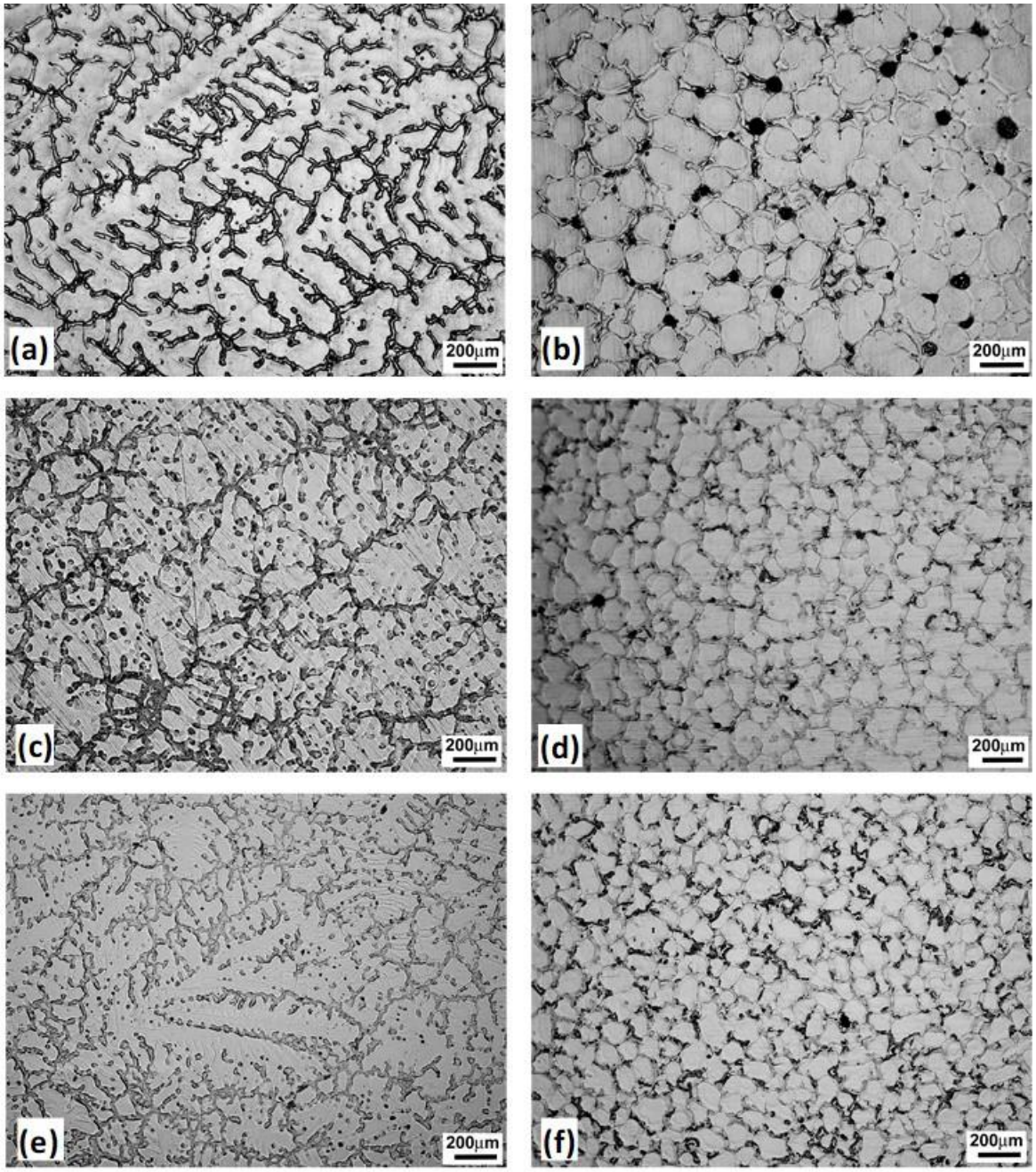

Fig. 1 Microstructures of Mg-alloys solidified without ultrasonication (a) AZ31, (c) AJ62, (e) AZ91, and under ultrasonication (b) AZ31, (d) AJ62, (f) AZ91.

Solidification microstructure of eutectics and intermetallics

Two alloy compositions representing a regular (Al-33Cu, all compositions expressed in wt.%) and an irregular (Al-16Si) eutectic were ultrasonicated. In the absence of ultrasonication, Al-33Cu shows a typical regular eutectic microstructure consisting of fully lamellar colonies as shown in Fig. 2a. Under ultrasonication, the lamellar eutectic degenerated into a duplex microstructure consisting of coarse and rounded Al_2Cu (dark) and α-Al (light) particles (Fig. 2b). Few isolated lamellar regions observed in the microstructure are presumed to be solidified at the end of solidification following the withdrawal of ultrasound. Degenerated microstructure was observed to be confined within 15mm from the radiator and beyond that the microstructure

rapidly reverted to lamellar eutectic with slightly increased lamellar spacing. Eutectic modification was also observed for the irregular eutectic in Al-16Si. Figs. 2c shows the microstructure formed without any ultrasonication consisting of blocky and faceted primary Si particles, long irregular eutectic Si plates embedded in α-Al matrix and complex Chinese script morphology of the α-AlFeSi intermetallic (IMC) particles. Under ultrasonication (Fig. 2d), the primary Si particles are significantly refined and better dispersed in the microstructure. More importantly, the long eutectic-Si plates have been entirely replaced with compact polygonal eutectic-Si particles. This was noticeable in an area 10mm around the radiator. The modification effect was diminished with distance from the radiator. Beyond 15mm, eutectic Si platelets formed gradually increasing in length with distance from the radiator. Similarly, α-AlFeSi IMC were observed to form as compact polygonal particles around the radiator. Unlike observed primary grain refinement throughout the ingots (albeit with better efficiency near the radiator), eutectic and IMC modification was predominantly confined near the radiator and the effect diminished rapidly with distance from the radiator.

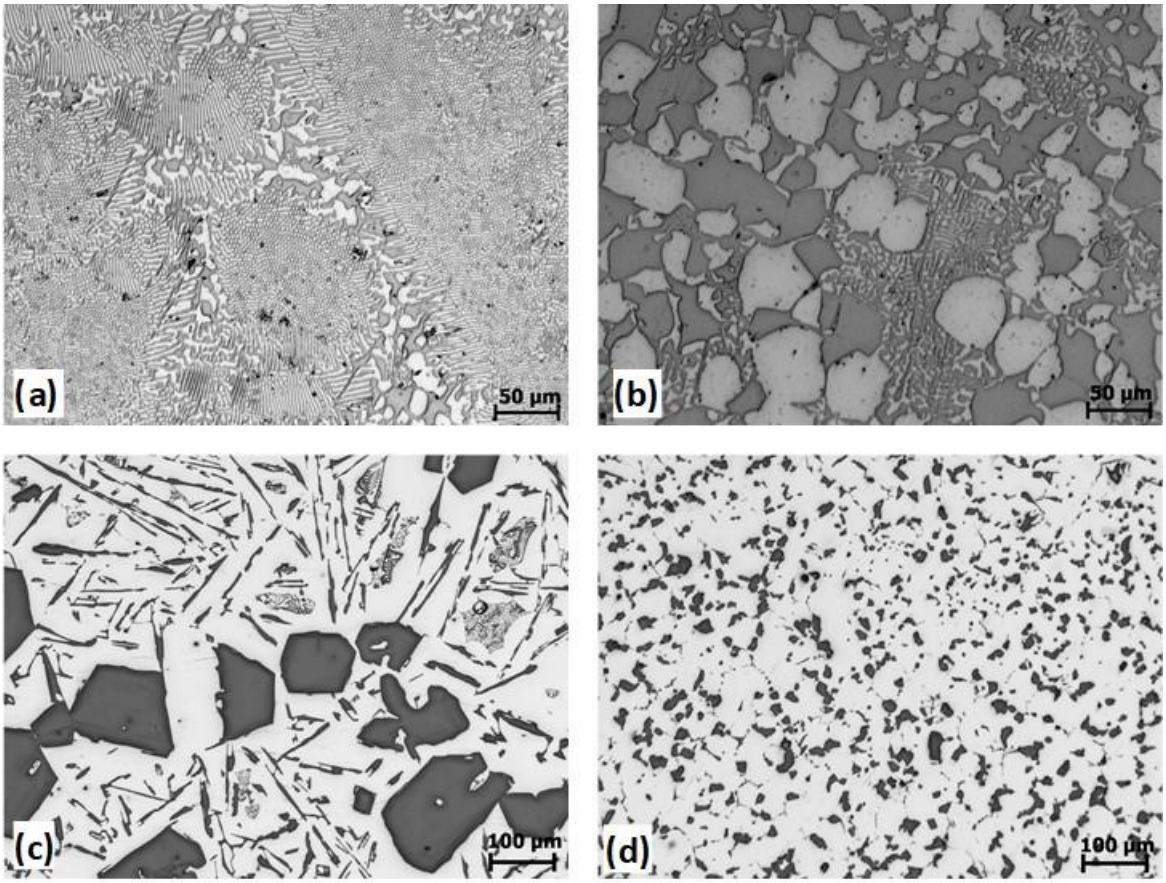

Fig. 2 Microstructures of eutectic alloys solidified without ultrasonication (a) Al-22Cu, (c) Al-16Si, and under ultrasonication (b) Al-33Cu, (d) Al-16Si.

Heat treatability of AZ80 solidified in the presence and absence of ultrasonication

Ultrasonicated AZ80 ingots showed a higher average hardness of 69 HV compared to conventionally solidified ingots at 55 HV in the as-cast condition. The increase in hardness could be related to grain refinement from ultrasonication. Following solution treatment at 400 ^{o}C for 6 h, the disparity in hardness reduced with the conventionally solidified and

ultrasonicated samples showing average hardness values of 59 HV and 65 HV, respectively. Both samples showed significant reduction in the intergranular β-phase ($Al_{17}Mg_{12}$) and eutectic areas following solution treatment, although ultrasonicated samples appeared to show slightly better dissolution of the second phase. The hardness trends observed in the samples are plotted in Fig. 3 for different aging temperatures and times. The ultrasonicated samples consistently showed slightly higher hardness compared to conventionally solidified samples. Although the peak hardness achieved in both types of sample appear similar, especially at higher temperature, ultrasonicated samples showed better age hardening response with higher hardness values at lower aging times and slower over-aging behaviour.

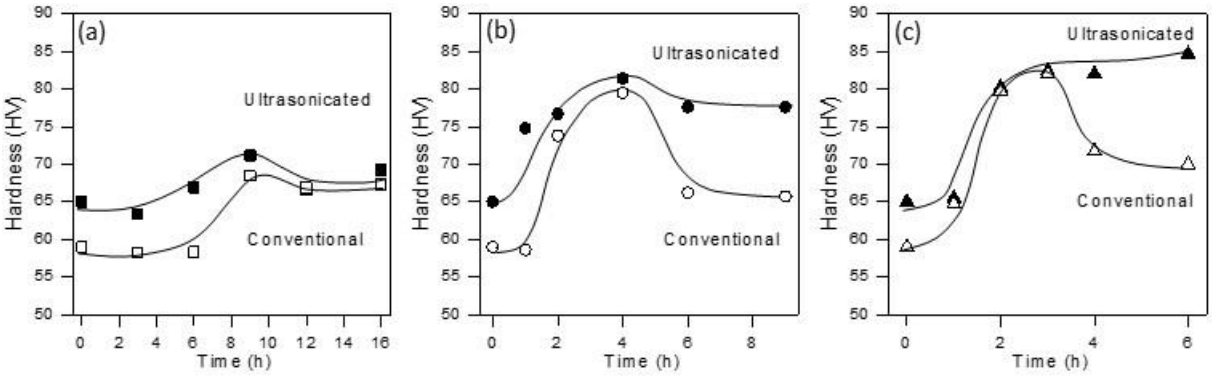

Fig. 3 Artificial aging curves for solution treated AZ80 (solidified with and without ultrasonication) at (a) 150 °C, (b) 200 °C and (c) 225 °C. Average hardness calculated from six indentions with outliers eliminated.

Microstructures from the samples aged at 225 °C for 6 h are presented in Figs. 4a and 4b for the conventionally solidified and ultrasonicated ingots, respectively. Both samples show predominantly discontinuous precipitation of lamellar β-phase from the grain boundaries, but a distinct difference is noted between the samples. While the precipitation only covers part of the grains (around the grain boundaries) in the conventionally solidified samples, grains in the ultrasonicated samples are almost completely covered by precipitates. As discontinuous precipitation initiates at the grain boundaries and proceeds towards the interior of the grains, it is evident that the kinetics of precipitation has enhanced following ultrasonication.

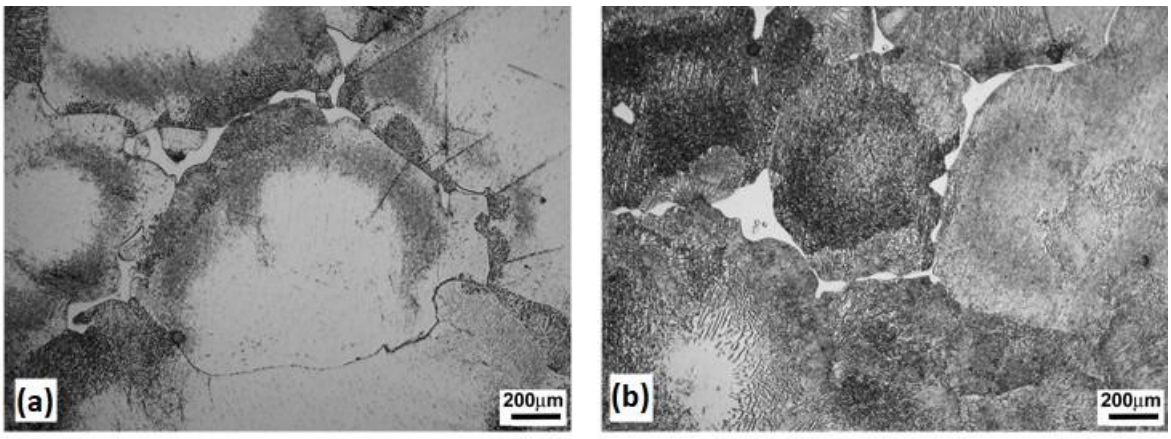

Fig. 4 Optical micrographs from AZ80 after solution treatment and artificial aging for 6 h at 225 °C in samples solidified (a) without and (b) under ultrasonication.

Discussion

Figure 1 demonstrates that ultrasonication significantly refines α-Mg grains compared to ingots solidified without ultrasonication in various Mg-alloys. Also, strongest refinement is noted near the radiator with progressive increase in grain size with distance as with previous reports. Nevertheless, the microstructure is non-dendritic and refined over the entire ingots under ultrasonication compared to conventionally solidified ingots. The effect of ultrasonication during solidification has been attributed to cavitation whereby instantaneous formation, growth and collapse of bubbles can create local shockwave (1000 atm) and strong microjet (100 m/s), and acoustic streaming creating bulk fluid flow due to the attenuation of ultrasound traveling through the melt [11]. The finest grain structure observed near the radiator (area of active cavitation) signifies major influence of cavitation on grain refining. Although cavitation diminishes away for the radiator, grain refinement observed in the entire ingots suggests that sufficient nuclei has been transported and redistributed into the bulk melt through acoustic streaming to promote refined non-dendritic microstructure for the ingot sizes solidified.

The type and amounts of solute greatly influence the grain size. Solute concentration at the solid-liquid interface is known to promote columnar-equiaxed transition and grain refinement through constitutional undercooling [20]. Correlation of solute with grain size is commonly achieved using the 'Growth Restriction Factor', Q, expressed as $Q = mC_0(1-k)$ where m is the slope of the liquidus curve, C_0 the alloy composition and k the solute distribution co-efficient according to the equilibrium phase diagram. Considering the growth of spherical crystals restricted by the partition of single solute, the crystal growth rate is proportional to the diffusivity of the solute, and inversely to Q. For multi-component alloys, the overall growth restriction factor is often computed by summing Q values of individual solutes as $Q = \sum_i m_i c_{0i} (k_i - 1)$. Figure 5 presents the average grain size (from near the radiator in ultrasonicated samples) as a function of the inverse of growth restriction factor, Q. A reduction in grain size with increased Q is observed from Fig. 5 indicating that grain refinement is assisted by solute effects under both conventional and ultrasound assisted solidification. While such solutal effect is well-established for conventional solidification, the result illustrates that strong fluid flow under cavitation does not diminish growth restriction effect of solute during solidification.

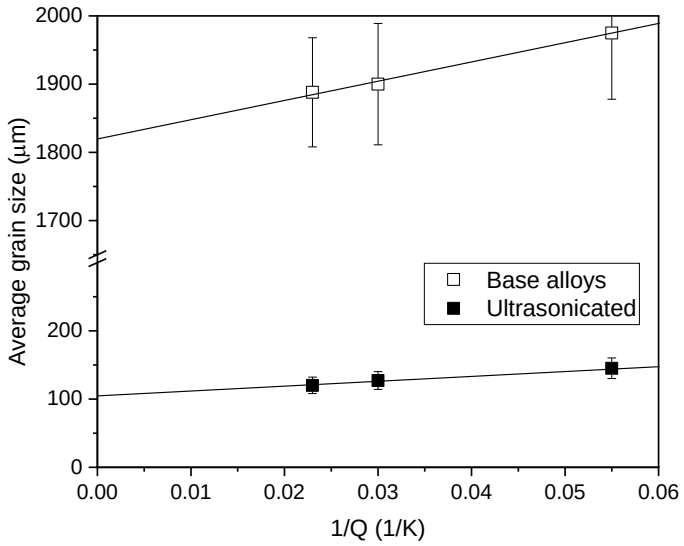

Fig. 5 Plot of average grain size against the inverse of growth restriction factor (Q) for AZ31, AJ62 and AZ91 alloys solidified in the presence and absence of ultrasonication.

A plot of grain size (d_{gs}) against 1/Q showing a linear relationship of the form $d_{gs} = a + b/Q$ can be qualitatively used to interpret heterogeneous nucleation activity during solidification. The intercept 'a' relates to the active nucleant density, with a lower intercept signifying larger number of nucleants in the melt. The slope 'b' is related to the potency of the nucleants, with a lower slope signifying higher nucleation potency [21]. It can be seen from Fig. 5 that both ultrasonicated and conventionally solidified samples follow perfect linear relationship between the average grain size and 1/Q. More importantly, the intercept 'a' for ultrasonicated samples (103.2 μm) is considerably lower than for conventionally solidified samples (1820.4 μm) suggesting more nucleating particles being present in the ultrasonicated melts. Similarly, the slope of the ultrasonicated samples (767.3 μmK) is noticeably lower than for conventionally solidified samples (2793.3 μmK) indicating higher potency of nucleating particles under ultrasonication. As the existing nucleating particles in the alloy melts are entirely indigenous, more nucleants under ultrasonication can only be generated from wetting of non-metallic inclusions or dendrite fragments. The increased nucleation potency under ultrasonication can be explained by the pressure pulse effect whereby the increase in the freezing point under cavitation can activate the nucleants through additional effective undercooling [22].

The secondary benefit of grain refinement under ultrasonication is improved age hardening response of the cast samples as evidenced in the present work. During solution treatment, dissolution of intergranular second phase (eutectic and precipitate) in the ultrasonicated samples is improved as the second phase network is uniformly dispersed in between the refined grain structure and aided by the reduced diffusion distance. Large grain size in the conventionally solidified ingots confined the second phase in coarser isolated pockets leading to poor dissolution (of the second phase) and solute homogenization in the grains within the solution treatment time. This further contributed to age hardening response of the samples. It has been

established that nature of precipitation in AZ80 alloys at lower temperature (as in the present investigation) is predominantly discontinuous [23]. For Mg-alloys with high Al content, it has been shown that the transportation of solute atoms during discontinuous reactions is governed by grain boundary diffusion [24]. The finer grain size in the ultrasonicated ingot enhances the precipitation kinetics by increasing the grain boundary area. This is evident in Fig. 4 where for identical aging treatment precipitation covers the entire grains in the ultrasonicated sample (Fig. 4b) as opposed to the conventionally solidified sample showing precipitation near the grain boundaries with precipitate free grain interiors (Fig. 4a). Apart from the reduction in grain boundary area in the conventionally solidified ingot, the lack of solute supersaturation in the grain interiors may also deter precipitation due to reduced driving force.

As observed in Fig. 2, both regular and irregular eutectic morphologies are altered under ultrasonication. However, unlike for primary grain refinement, the modification effect is confined mostly around the radiator in the area of active cavitation. The degeneration of regular lamellar eutectic microstructure in Al-33Cu is indicative of breakdown of growth cooperation between the phases that is likely if the coupled diffusion geometry is disturbed. Chemical modification of Al-Si eutectic is generally associated with reduced eutectic-Si nucleation and suppression of eutectic temperature (increased nucleation undercooling). Nucleation enhancement under ultrasonication cannot explain the observed eutectic modification. Therefore, modification of eutectic morphology appears to be growth related and originates from solute homogenisation at the eutectic growth front leading to coarsening and spheroidisation. Considering that solutal diffusion boundary layer existing at the eutectic growth front is extremely thin (of the order of lamellar spacing), disturbing this diffusion layer would require extremely intense convection. This is possible under the shockwave created through cavitation and explains why the degeneration and spheroidisation of eutectic is only prominent over a short distance (about 15mm) around the radiator. Fluid flow in the bulk melt from acoustic streaming is not strong enough to alter the diffusion geometry for eutectic growth and the modification effect rapidly deteriorates with increased distance from the radiator.

Conclusions

Ultrasonication during the solidification of Mg-alloys AZ31, AZ91 and AJ62 shows extensive grain refinement. Grain sizes are finest near the radiator and increases progressively with distance, although the entire ingot (for the sizes investigated) shows refined equiaxed grain structure compared to large dendritic grains observed in the conventionally solidified ingots.

A direct correlation between the average grain size and the solute growth restriction factor has been observed in the alloys indicating that strong fluid flow under ultrasonication does not diminish the growth restriction effect of solute.

Heat treatability involving both solution treatment and artificial aging is observed to enhance in ultrasonicated AZ80 as compared to conventionally solidified samples. Enhanced dissolution and accelerated discontinuous precipitation of second phase results from the grain refinement and increased grain boundary area in the ultrasonicated samples.

Regular lamellar eutectic in Al-33Cu shows degeneration and irregular eutectic Si-plates in Al-16Si are replaced with compact polygonal particles in the areas around the ultrasound radiator. Complex Chinese-script intermetallic were also modified to compact polygonal particles in this area of active cavitation.

Grain refinement under ultrasonication appears to originate from enhanced nucleation indicating an increase in the number and potency of nucleating agents while eutectic and intermetallic modification seems to be a growth phenomenon caused by coarsening and spheroidisation under the strong fluid flow from cavitation.

Acknowledgment
Dr Hiren Kotadia thanks the support of WMG— High Value Manufacturing Catapult.

References

[1] Spittle JA (2006) Columnar to equiaxed grain transition in as solidified alloys. Int. Mater. Rev. 51(4):247–269. doi: 10.1179/174328006X102493.
[2] Murty BS, Kori SA, Chakraborty M (2002) Grain refinement of aluminium and its alloys by heterogeneous nucleation and alloying. Int. Mater. Rev. 47(1):3–29. doi: 10.1179/095066001225001049.
[3] Greer AL, Cooper PS, Meredith MW, Schneider W, Schumacher P, Spittle JA, Tronche A (2003) Grain refinement of aluminium alloys by inoculation, Adv. Eng. Mater. 5(1-2):81–91. doi: 10.1002/adem.200390013.
[4] Qian M, StJohn DH, Frost MT (2004) Heterogeneous nuclei size in magnesium–zirconium alloys. Scr. Mater. 50(8):1115-1119. doi: 10.1016/j.scriptamat.2004.01.026.
[5] Ali Y, Qiu D, Jiang B, Pan F, Zhang MX (2015) Current research progress in grain refinement of cast magnesium alloys: a review article. J. Alloys Compd. 619:639–651. doi: 10.1016/j.jallcom.2014.09.061.
[6] Lu SZ, Hellawell A (1995) Modification of Al-Si alloys: Microstructure, thermal analysis, and mechanisms. JOM 47(2):38-40. doi: 10.1007/BF03221405.
[7] Easton MA, Qian M, Prasad A, StJohn DH (2016) Recent advances in grain refinement of light metals and alloys. Curr. Opin. Solid State Mater. Sci. 20(1):13–24. doi: 10.1016/j.cossms.2015.10.001.
[8] Das A, Liu G, Fan Z (2006) Investigation on the microstructural refinement of an Mg-6wt.% Zn alloy. Mater. Sci. Eng. A419:349-356. doi: 10.1016/j.msea.2006.01.023.
[9] Vives C (1989) Electromagnetic refining of aluminum alloys by the CREM process: Part I. Working principle and metallurgical results. Metall. Trans. B. 20(5):623-629. doi: 10.1007/BF02655919.
[10] Räbiger D, Zhang Y, Galindo V, Franke S, Willers B, Eckert S (2014) The relevance of melt convection to grain refinement in Al–Si alloys solidified under the impact of electric currents. Acta Mater. 79:327-338. doi: 10.1016/j.actamat.2014.07.037.
[11] Eskin GI, Eskin DG (2015) Ultrasonic treatment of light alloy melts, 2nd Ed. CRC Press, Boca Raton.

[12] Kotadia HR, Qian M, Eskin DG, Das A (2017) On the microstructural refinement in commercial purity Al and Al-10wt% Cu alloy under ultrasonication during solidification. Mater. Des. 132:266–274. doi: 10.1016/j.matdes.2017.06.065.

[13] Atamanenko TV, Eskin DG, Zhang L, Katgerman L (2010) Criteria of grain refinement induced by ultrasonic melt treatment of aluminum alloys containing Zr and Ti. Metall. Mater. Trans. A. 41 (8), 2056-2066. doi: 10.1007/s11661-010-0232-4.

[14] Wang G, Dargusch MS, Qian M, Eskin DG, StJohn DH (2014) The role of ultrasonic treatment in refining the as-cast grain structure during the solidification of an Al–2Cu alloy. J. Cry. Growth 408, 119-124. doi: 10.1016/j.jcrysgro.2014.09.018.

[15] Qian M, Ramirez A, Das A (2009) Ultrasonic refinement of magnesium by cavitation: clarifying the role of wall crystals. J. Cryst. Growth. 311(14):3708-3715. doi: 10.1016/j.jcrysgro.2009.04.036.

[16] Liu X, Osawa Y, Takamori S, Mukai T (2008) Grain refinement of AZ91 alloy by introducing ultrasonic vibration during solidification. Mater. Lett. 62 (17–18), 2872-2875. doi: 10.1016/j.matlet.2008.01.063.

[17] D Gao, Z Li, Q Han, Q Zhai (2009) Effect of ultrasonic power on microstructure and mechanical properties of AZ91 alloy, Mat. Sci. Eng. A, 502 (1–2) 2-5. doi: 10.1016/j.msea.2008.12.005.

[18] Das A, Kotadia HR (2011) Effect of high-intensity ultrasonic irradiation on the modification of solidification microstructure in a Si-rich hypoeutectic Al–Si alloy. Mater. Chem. Phys. 125(3):853-859. doi: 10.1016/j.matchemphys.2010.09.035.

[19] Abramov V, Abramov O, Bulgakov V, Sommer F (1998) Solidification of aluminium alloys under ultrasonic irradiation using water-cooled resonator, Mater. Lett. 37 (1-2), 27-34. doi: 10.1016/S0167-577X(98)00064-0.

[20] Spittle JA (2006) Columnar to equiaxed grain transition in as solidified alloys. Int. Mater. Rev. 51(4):247-269. doi: 10.1179/174328006X102493.

[21] StJohn DH, Qian M, Easton MA, Cao P, Hildebrand Z (2005) Grain refinement of magnesium alloys. Metall. Mater. Trans. A. 36(7):1669-1679. doi: 10.1007/s11661-005-0030-6.

[22] Hunt JD, Jackson KA (1966) Nucleation of Solid in an undercooled liquid by cavitation. J. Appl. Phys. 37(1):254-257. doi: 10.1063/1.1707821.

[23] Yu S, Gao Y, Liu C, Han X (2015) Effect of aging temperature on precipitation behavior and mechanical properties of extruded AZ80-Ag alloy. J. Alloys Comp. 646:431-436. doi: 10.1016/j.jallcom.2015.06.126.

[24] Bradai D, Kadi-Hanifi M, Zieba P, Kuschke WM, Gust W (1999) The kinetics of the discontinuous precipitation and dissolution in Mg-rich Al alloys. J. Mater. Sci. 34:5331–5336. doi: 10.1023/A:1004753122411.